DETERMINATION OF FAN DESIGN PARAMETERS FOR LIGHT-SPORT AIRCRAFT

JAN KLESA

Czech Technical University, Faculty of Mechanical Engineering, Department of Aerospace Engineering,
Karlovo náměstí 13, Prague 2, Czech Republic

correspondence: `jan.klesa@fs.cvut.cz`

ABSTRACT. This paper is focused on the preliminary design of an electric fan for light-sport aircraft. Usage of electric motors brings some advantages compared to piston engines, especially small size and the independence of power on shaft RPM. A 1D compressible fluid flow model is used for the determination of the performace. The influence of various system parameters is analysed. Results for the case of the UL-39 ultralight aircraft are presented. Finally, input parameters for the fan design are determined according to this analysis. This can be then used as input data for the standard fan (axial compressor) design procedure.

KEYWORDS: Ducted fan, electric propulsion, axial compressor.

1. INTRODUCTION

Electric propulsion for aircrafts became a research topic in the last years, which is motivated by the huge progress in low-weight electric power systems. Electric flight was already developed in the 1960s for radio controlled model aircraft, e.g., work of Fred Militky [1]. The progress in battery technology (from NiCd to lithium-based batteries), electric motors (from simple DC brush motors with ferrite magnets, later neodymium magnets, and today brushless DC motors) and control electronics led to the increase of model performance and size.This led to the possibility of building manned electrical aircrafts in the last decade, e.g., projects of Airbus, Pipistrel, Extra, Jihlavan, etc.

Today, the technology is advanced enough to build a small fully-electric aircraft. The electric propulsion brings some advantages, especially possible drag reduction due to the lower volume and cross-section of electric motors in comparison with turboprop and piston engines. This allows to decrease the nacelle size (for multiple engine aircraft) and better fuselage nose shape (for single engine aircraft). However, cooling the electric components requires relatively large cooling systems because of the low temperature difference. The main disadvantage remains the source of the electric energy. Batteries are relatively heavy and have a low energy density as compared with aircraft fuel [1]. Another problem is the long time necessary for recharging the batteries between flights. Refuelling is usually much faster and does not require a high power electric line connection at the airport. Thus, some hybrid system using standard aircraft fuel (e.g., Jet-A1) or hydrogen is necessary for a long range/high endurance aircraft. In this case, electricity is made onboard by means of an electric generator powered by turboshaft engine or APU. In this case, energy can be stored in the high energy density medium, but the overall efficiency is lower due to the chain of necessary energy transformations. Both systems are under development for use in aviation, e.g., Honeywell [2] or Rolls-Royce [3].

A ducted fan is used on electric-powered "jet" aircraft, e.g., Airbus E-Fan. A ducted fan allows the transformation of the electric energy to the propulsive thrust at high flight velocity, where a propeller is inefficient. It became a dynamic research area in the last years due to the efforts of building electric or hybrid-electric transport aircrafts.

However, ducted fans or ducted propellers have a lower performance at low flight speeds for multiple reasons:

- Higher outlet velocity which causes lower propulsive efficiency.
- Higher losses in the propulsion system due to the friction at duct walls.
- Higher fuselage (nacelle) drag.
- Higher drag when flying with the engine off-regime.

But there is also some motivation for fan-powered low-speed aircraft, which can have various advantages:

- Safety, because rotating parts are covered by the duct, and so the risk of damage or injures can be lower than for a conventional propeller.
- Possible noise reduction.
- "Jet-feeling" - fan-powered aircraft can be used for low-cost training of jet pilots.

The preliminary design and a comparison of a ducted fan with a propeller was presented in [4]. This paper is based on the experience with the long developement of the UL-39 aircraft at the Department of Aerospace Engineering of the Czech Technical University in Prague. A more general approach with a compressible fluid flow model is used, which means
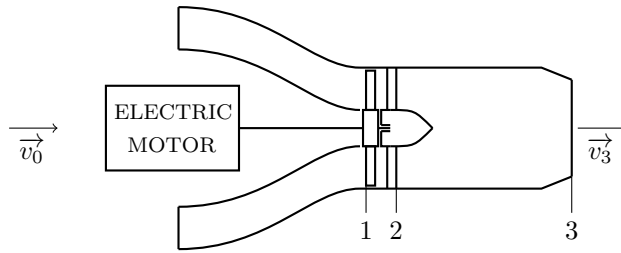
FIGURE 1. Propulsion system scheme.

Free atmosphere	0
Plane in front of the fan	1
Plane behind the fan	2
Nozzle exit	3

TABLE 1. Section definitions.

that this approach can also be used for a much faster aircraft than the UL-39.

The aircraft and also its propulsion system must fullfill legal requirements. For Czech ultalight aircraft, it is certification specification UL-2 [5] (requirements of the German certification specification LTF-UL are very similar [6]). This brings the requirement that the aircraft has to take-off on a given distance, this creates requirement for thrust at low speeds so that the acceleration is adequate.

2. METHODS

The simulation model is based on a modified approach from [4] based on experience from the developement and testing of the UL-39 aircraft. A compressible fluid model is used so that this method can be used for a faster aircraft than the ultralight cathegory. An approach to the fan design based on the comparison of various configurations for the complete flight velocity envelope is used due to certification specification requirements, which are contradictory to the requirement of high cruise speed as shown later in this paper, and led to the necessary modification of the approach presented in [4]. An iterative method in MATLAB is used for the solution of the system of equations. The result of the method is the fan design point which can then be used for the fan design by standard procedures, see e.g. [7] and [8].

2.1. PHYSICAL MODEL
The aim of the first step is to find parameters of the propulsion system in design conditions, which were determined according to the experience with the UL-39 aircraft testing and operation [9]. It is a 1D compressible fluid flow model. Input parameters used for the fan design phase can be found in Table 2. The fan has to be placed into the available space in the fuselage, which limits the maximal fan diameter and determines the length of the exhaust duct. Figure 1 and Table 1 explain the numbering of different planes in the propulsion system.

Due to the complexity of the equations, a numerical iterative approach is used for the solution. Input parameters are the fan diameter D_1 and nozzle cross-section ratio A_1/A_3. The thrust curve, i.e. dependence of the thrust T on the flight velocity v_0, is then determined for every combination of D_1 and A_1/A_3. The fan hub-to-tip radius ratio is set to 0.5, i.e. the

Engine power P	200 kW
Flight velocity range v_0	0–100 m s^{-1}
Air density ρ	1.225 kg m^3
Atmospheric pressure p_{s0}	101 325 Pa
Intake duct pressure loss coefficient ζ_{01}	0.1
Fan efficiency η_{fan}	0.85
Outlet duct wall friction factor λ_{23}	0.013
Outlet duct length L	1.5 m
Air ratio of specific heats κ	1.4
Air specific gas constant r	287 J kg^{-1} K^{-1}
Air specific heat at constant pressure c_p	1004.5 J kg^{-1} K^{-1}

TABLE 2. Input parameters for the propulsion system.

blade length is half of the fan radius. Then the fan cross-section A_1 can be determined according to

$$A_1 = \frac{3}{4}\frac{\pi D_1^2}{4}. \tag{1}$$

The total pressure in the free atmosphere in front of the aircraft is detemined by the standard formula from flight Mach number M_0 by

$$p_{t0} = p_{s0}(1 + \frac{\kappa - 1}{2}M_0^2)^{\frac{\kappa}{\kappa-1}}, \tag{2}$$

where the flight Mach number M_0 is

$$M_0 = \frac{v_0}{a_0} \tag{3}$$

and the speed of sound in the atmosphere a_0 is

$$a_0 = \sqrt{\kappa r T_{s0}}. \tag{4}$$

The total temperature can be deremined in a similar way

$$T_{t0} = T_{s0}\left(1 + \frac{\kappa - 1}{2}M_0^2\right). \tag{5}$$

The total pressure in the intake duct is computed by means of a loss coefficient ζ_{01} and the fan axial velocity v_1

$$p_{t1} = p_{t0} - \frac{\zeta_{01}\rho_1 v_1^2}{2}, \tag{6}$$

where $\zeta_{01} = 0.1$ (based on CFD simulations from [10]). The total pressure recovery coefficient (see [11]) cannot be used in this case due to the low flight speed (data from literature sources are suitable for a faster aircraft). Heat exchange in the intake duct is neglected, thus the total temperature remains the same

$$T_{t1} = T_{t0}. \tag{7}$$

The static temperature in front of the fan is

$$T_{s1} = T_{t1} - \frac{v_1^2}{2c_p}, \tag{8}$$

the speed of sound is then

$$a_1 = \sqrt{\kappa r T_{s1}}, \tag{9}$$

and the Mach number

$$M_1 = \frac{v_1}{a_1}. \tag{10}$$

The static pressure can then be calculated from the Mach number

$$p_{s1} = p_{t1} \left(1 + \frac{\kappa - 1}{2} M_1^2 \right)^{-\frac{\kappa}{\kappa - 1}}. \tag{11}$$

The density and the air mass flow are then computed according to

$$\rho_1 = \frac{p_{s1}}{r T_{s1}}, \tag{12}$$

$$\dot{m}_1 = \rho_1 v_1 A_1. \tag{13}$$

It is assumed that the whole engine power P is used by the fan, i.e. the total temperature is increased in the following way

$$T_{t2} = T_{t1} + \frac{P}{c_p \rho_1 A_1 v_1}. \tag{14}$$

The total temperature for isentropic compression due to the fan is

$$T_{t2i} = T_{t1} + \frac{\eta_{Fan} P}{c_p \rho_1 A_1 v_1}. \tag{15}$$

Then, the total pressure becomes

$$p_{t2} = p_{t1} \left(\frac{T_{t2i}}{T_{t1}} \right)^{\frac{\kappa}{\kappa - 1}}, \tag{16}$$

and the fan pressure ratio is

$$\Pi_{12} = \frac{p_{t2}}{p_{t1}}. \tag{17}$$

The stagnation density behind the fan is

$$\rho_{t2} = \frac{p_{t2}}{r T_{t2}}. \tag{18}$$

The critical air density (for choked flow state) behind the fan is

$$\rho_{c2} = \rho_{t2} \left(\frac{\kappa + 1}{2} \right)^{-\frac{1}{\kappa - 1}}, \tag{19}$$

and the corresponding critical velocity is

$$v_{c2} = \sqrt{\frac{2 (\kappa - 1) c_p T_{t2}}{\kappa + 1}}, \tag{20}$$

and then, the critical flow density is

$$(\rho v)_{c2} = v_{c2} \rho_{c2}. \tag{21}$$

M_2 is computed so that the mass flow through the duct remains constant. i.e. $(\rho v)_1 = (\rho v)_2$. The speed of sound behind the fan is

$$a_2 = v_{c2} \sqrt{\frac{\kappa + 1}{2} \left(1 + \frac{\kappa - 1}{2} M_2^2 \right)^{-1}}. \tag{22}$$

Then, the flow velocity is calculated from the Mach number M_2

$$v_2 = M_2 a_2, \tag{23}$$

and the air density becomes

$$\rho_2 = \rho_{t2} \left(1 + \frac{\kappa - 1}{2} M_2^2 \right)^{-\frac{1}{\kappa - 1}}. \tag{24}$$

The total pressure at the nozzle exit 3 is computed from the exhaust duct loss coefficient ζ_{23}

$$p_{t3} = p_{t2} - \zeta_{23} \frac{\rho_2 v_2^2}{2}. \tag{25}$$

The value of the loss coefficient ζ_{23} is determined according to the information from [12]. The flow density at the nozzle exit is computed from the condition of constant mass flow

$$(\rho v)_3 = \frac{(\rho v)_2}{\frac{A_3}{A_1}}. \tag{26}$$

The total temperature behind the fan remains constant

$$T_{t3} = T_{t2}. \tag{27}$$

The total air density at the nozzle exit is

$$\rho_{t3} = \frac{p_{t3}}{r T_{t3}}. \tag{28}$$

The critical (choked) air density in the nozzle exit is

$$\rho_{c3} = \rho_{t3} \left(\frac{\kappa + 1}{2} \right)^{-\frac{1}{\kappa - 1}}, \tag{29}$$

and the corresponding critical air velocity is

$$v_{c3} = \sqrt{\frac{2 (\kappa - 1) c_p T_{t3}}{\kappa + 1}}, \tag{30}$$

and the critical flow density is

$$(\rho v)_{c3} = \rho_{c3} v_{c3}. \tag{31}$$
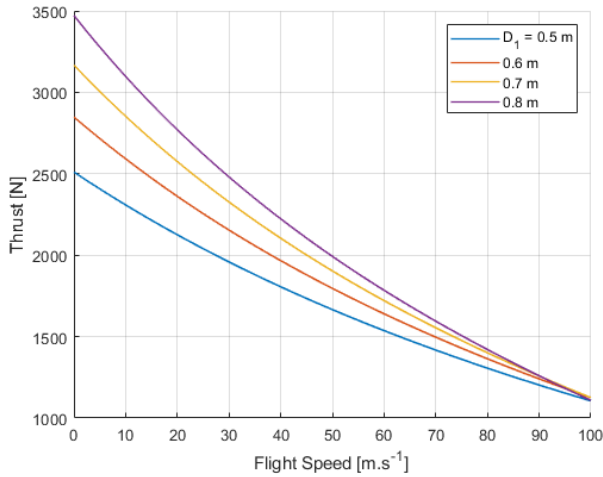
FIGURE 2. Thrust over flight speed for different fan diameters D_1, nozzle contraction ratio $A_1/A_3 = 1$.

FIGURE 3. Thrust over flight speed for different nozzle contraction ratios A_1/A_3, fan diameter $D_1 = 0.66\,\mathrm{m}$.

The static temperature in the nozzle exit is

$$T_{s3} = T_{t3} \left(\frac{p_{s0}}{p_{t3}} \right)^{\frac{\kappa - 1}{\kappa}}, \qquad (32)$$

the corresponding speed of sound is

$$a_3 = \sqrt{\kappa r T_{s3}}, \qquad (33)$$

and the flow velocity is

$$v_3 = M_3 a_3. \qquad (34)$$

The nozzle exit Mach number M_3 is determined from the relation between static pressure p_{s3} and total pressure p_{t3}

$$p_{s3} = p_{t3} \left(1 + \frac{\kappa - 1}{2} M_3^2 \right)^{-\frac{\kappa}{\kappa - 1}}. \qquad (35)$$

The thrust of the propulsion system is determined from the momentum conservation law

$$T = \dot{m} \left(v_3 - v_0 \right), \qquad (36)$$

where the air mass flow is

$$\dot{m} = \rho_1 A_1 v_1. \qquad (37)$$

Finally, the propulsion efficiency is defined by the standard formula

$$\eta = \frac{T v_0}{P}. \qquad (38)$$

An iterative algorithm has to be used for the computation . A value $v_1 = 50\,m\,s^{-1}$ can be used as a guess for the first iteration.

Fan RPM is determined from the flow coefficient $\phi = v_{ax}/u$ which is assumed to be 0.5

$$n_m = \frac{120 v_1}{\pi D_1}. \qquad (39)$$

3. RESULTS

Thrust cuves (i.e. dependence of the thrust on the flight velocity) for different fan diameters D_1 and nozzle contraction ratios A_1/A_3 are presented in Figures 2 and 3. An increase in fan diameter D_1 (see Figure 2) causes a thrust increase for the given velocity range, however, this influence diminishes with increasing flight velocity as expected from the general theory of aerospace propulsion. The influence of nozzle contraction ratios A_1/A_3 on thrust (see Figure 3) is similar. Lower A_1/A_3 leads to a higher thrust at a lower flight velocity, but reduces the flight performance at a higher velocity. The influence of the fan diameter D_1 and nozzle contraction ratio A_1/A_3 on the efficiency is presented in Figures 4 and 5. The efficiency is relatively low in comparison with the standard propeller due to the small fan cross-section area and also due to the viscous losses in the duct system.

Another important parameter for the fan design is the axial velocity v_1 presented in Figures 6 and 7. It is clearly visible that there is a strong dependence of the fan axial velocity v_1 on constant electric motor power. Both parameters, i.e. fan diameter D_1 and nozzle contraction ratio A_1/A_3, have a strong influence on v_1. The dependence of the fan pressure ratio on the flight velocity and fan diameter is presented in Figure 8. The fan RPM for the same situation is presented in Figure 9 (the assumption of constant $\phi = v_{ax}/u = 0.5$ is used).

Based on the above-mentioned results, the dependencies of fan pressure ratio Π, thrust T, fan axial velocity v_1 and fan RPM n_m on the fan diameter D and nozzle contraction ratio A_1/A_3 for static case (i.e. $v_0 = 0\,\mathrm{km\,h^{-1}}$, take-off) and for maximum flight velocity (i.e. $v_0 = 300\,\mathrm{km\,h^{-1}}$), are presented in Figures 10–17. Based on this and the fuselage geometry, a fan diameter of $D_1 = 0.66\,\mathrm{m}$ was selected. The ratio A_1/A_3 is determined from the relative thrust shown in Figure 18. The relative thrust is defined as the ratio T/T_{ref}, where the reference value T_{ref} is
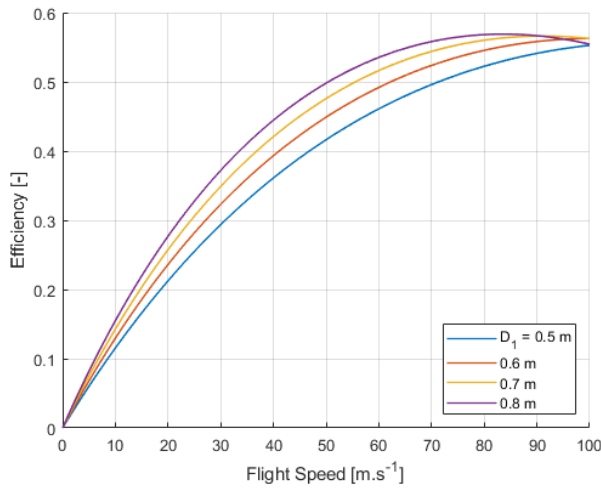
FIGURE 4. Efficiency of the propulsion system for different fan diameters D_1, nozzle contraction ratio $A_1/A_3 = 1$.
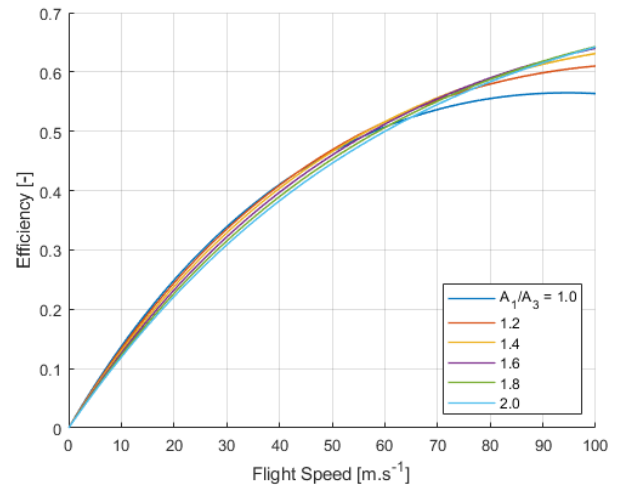
FIGURE 5. Efficiency of the propulsion system for different nozzle contraction A_1/A_3, fan diameter $D_1 = 0.66$ m.
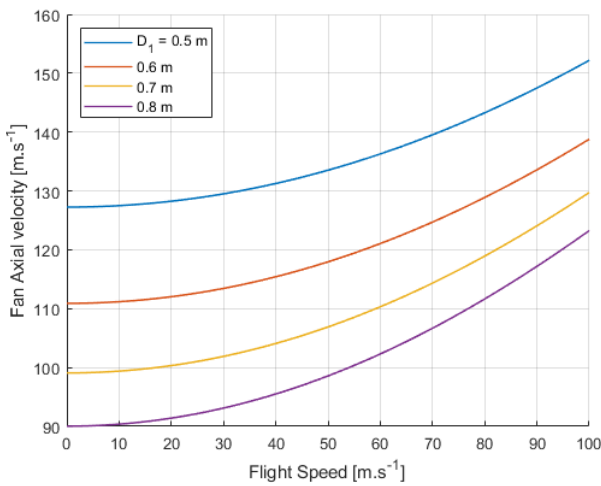
FIGURE 6. Fan axial velocity component over flight speed for different fan diamenters and $A_1/A_3 = 1$.
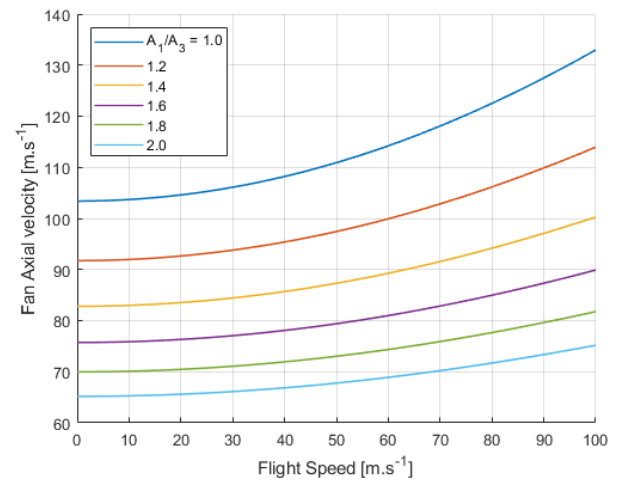
FIGURE 7. Fan axial velocity component over flight speed for different nozzle contraction ratios A_1/A_3, fan diameter $D_1 = 0.66$ m.
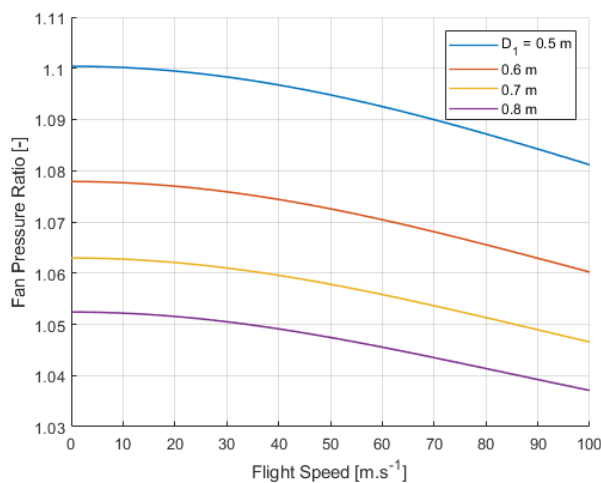
FIGURE 8. Fan pressure ratio over flight speed for different fan diamenters and $A_1/A_3 = 1$.
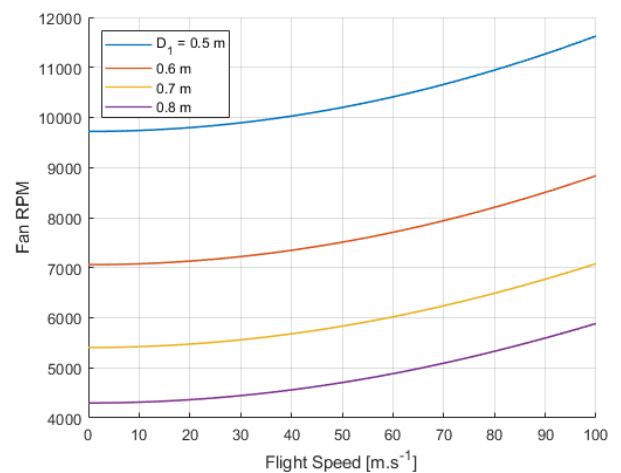
FIGURE 9. Fan RPM over flight speed for different fan diamenters and $A_1/A_3 = 1$.
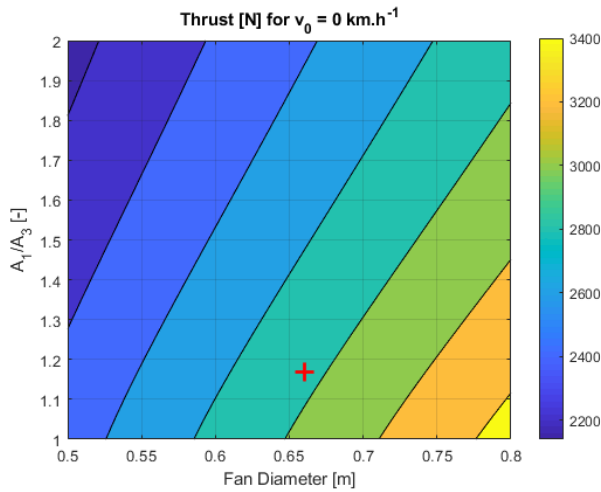
FIGURE 10. Dependence of static thrust on fan diameter and nozzle contraction ratio A_1/A_3. The selected fan design point parameters are marked by red cross.
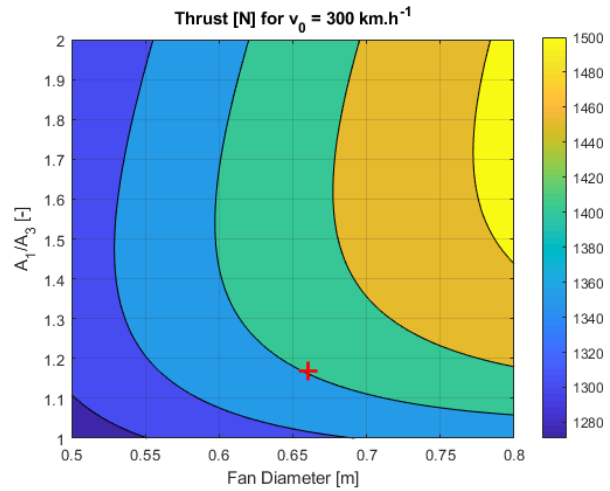
FIGURE 11. Dependence of thrust at flight speed $v_0 = 300\,\mathrm{km\,h^{-1}}$ on fan diameter and nozzle contraction ratio A_1/A_3. The selected fan design point parameters are marked by red cross.
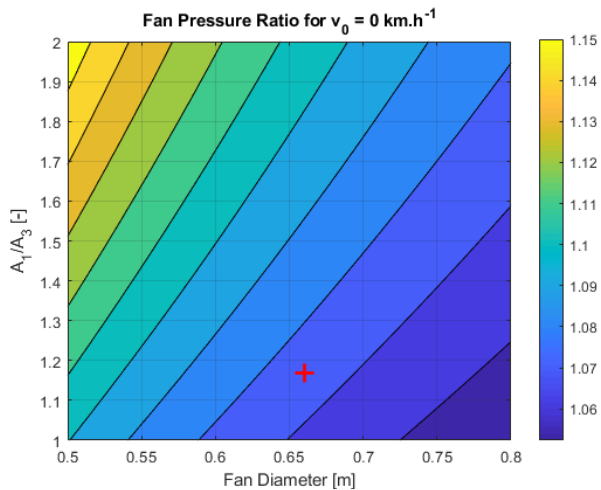
FIGURE 12. Dependence of fan pressure ratio at flight speed $v_0 = 0\,\mathrm{km\,h^{-1}}$ on fan diameter and nozzle contraction ratio A_1/A_3. The selected fan design point parameters are marked by red cross.
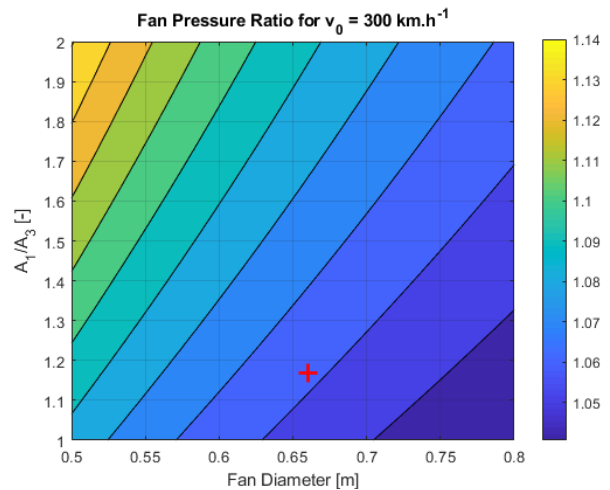
FIGURE 13. Dependence of fan pressure ratio at flight speed $v_0 = 300\,\mathrm{km\,h^{-1}}$ on fan diameter and nozzle contraction ratio A_1/A_3. The selected fan design point parameters are marked by red cross.

the maximum thrust for each velocity. The optimal value is the maximum of relative thrust mean value for flight velocity $0\,\mathrm{km\,h^{-1}}$ and $300\,\mathrm{km\,h^{-1}}$. This gives an optimal value of A_1/A_3 equal to 1.17. The resulting performance of the propulsion system is then determined for this case, see Figures 19 and 20. Also, the dependence of the fan design parameters on the flight velocity is computed, i.e. fan pressure ratio Π in Figure 21, fan axial velocity v_0 in Figure 22 and fan RPM n_m in Figure 23.

4. DISCUSSION

The presented results show that the high static thrust requirement is in conflict with the high cruise speed requirement (i.e. high thrust at high flight velocity) as expected from the general aircraft propulsion theory. This is clearly visible in Figure 18. The UL-39

light-sport aircraft is used as an example for this computation; the results for similar aircrafts are expected to be comparable. That is why the optimal system configuration is set by means of relative thrust. The outputs of this method are the fan design parameters presented in Table 3.

5. CONCLUSIONS

The results of the propulsion system simulation for ducted fan aircraft are presented. A compressible fluid flow model is used so the described procedure can be used for a wider range of flight velocities in comparison with a simple, incompressible flow model (e.g. [4]). The procedure is described and results are presented for the example of the UL-39 aircraft. The requirements for the propulsion system are contradictory, i.e. short take-off distance and high maximal
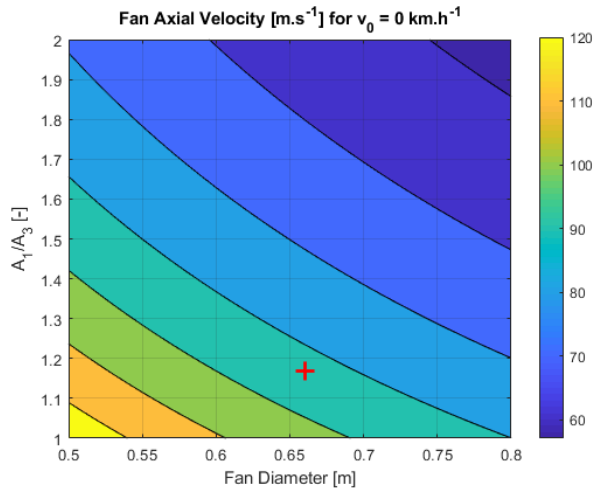
FIGURE 14. Dependence of fan axial velocity component at flight speed $v_0 = 0\,\mathrm{km\,h^{-1}}$ on fan diameter and nozzle contraction ratio A_1/A_3. The selected fan design point parameters are marked by red cross.
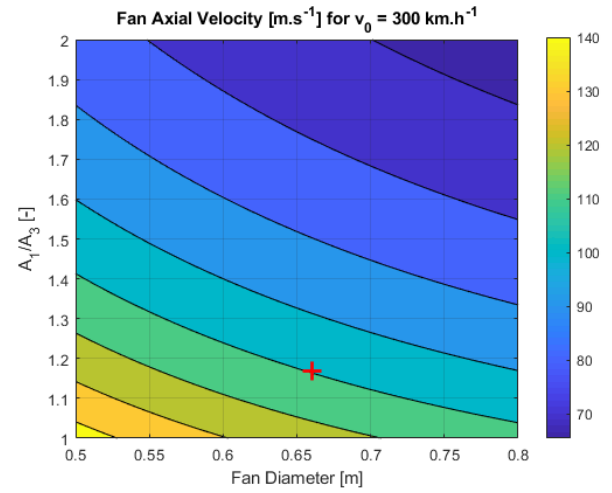
FIGURE 15. Dependence of fan axial velocity component at flight speed $v_0 = 300\,\mathrm{km\,h^{-1}}$ on fan diameter and nozzle contraction ratio A_1/A_3. The selected fan design point parameters are marked by red cross.
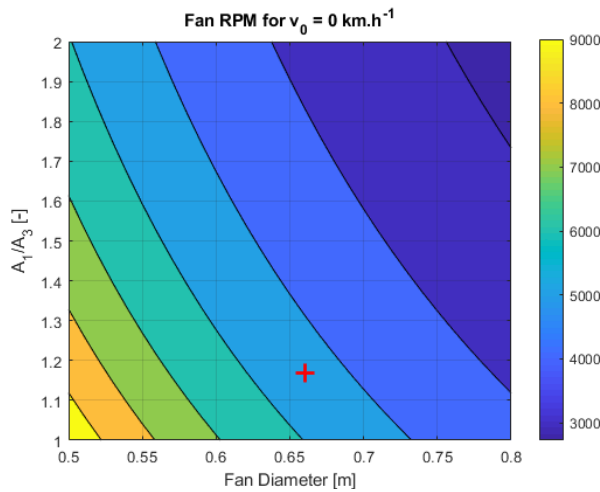
FIGURE 16. Dependence of fan RPM at flight speed $v_0 = 0\,\mathrm{km\,h^{-1}}$ on fan diameter and nozzle contraction ratio A_1/A_3. The selected fan design point are marked by red cross.
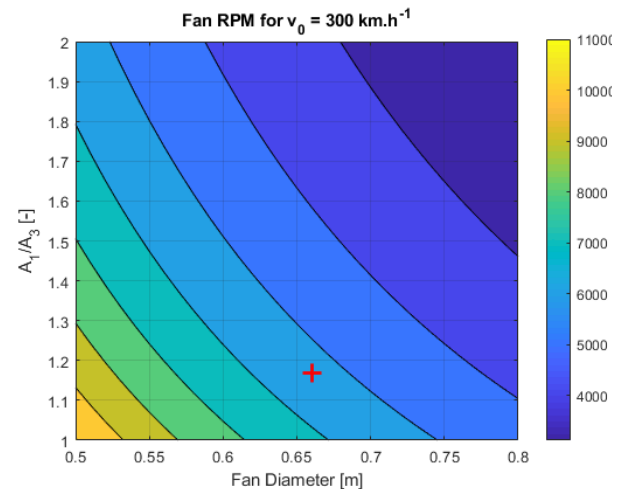
FIGURE 17. Dependence of fan RPM at flight speed $v_0 = 300\,\mathrm{km\,h^{-1}}$ on fan diameter and nozzle contraction ratio A_1/A_3. The selected fan design point parameters are marked by red cross.

Fan pressure ratio Π	1.062
Fan diameter D	660 mm
Electric motor RPM	6340
Air axial velocity at fan v_{ax}	$109.54\,\mathrm{m\,s^{-1}}$
Fan air mass flow $\dot{m}$	$33.46\,\mathrm{kg\,s^{-1}}$
Expected thrust at $300\,\mathrm{km\,h^{-1}}$ T	1401.9 N
Expected efficiency at $300\,\mathrm{km\,h^{-1}}$ η	0.584

TABLE 3. UL-39 fan design parameters for flight speed $300\,\mathrm{km\,h^{-1}}$ at sea level international standard atmosphere and electric motor power 200 kW.

flight velocity. This leads to the necessity of a trade-off for chosing the optimal system configuration. The influence of various design parameters on the propulsion performance is presented for the expected range of flight velocities. The proposed selection of the optimal variant is based on the maximum of mean relative thrust for the static case (i.e. flight velocity of $0\,\mathrm{km\,h^{-1}}$) and the expected high speed cruise (i.e. flight velocity of $300\,\mathrm{km\,h^{-1}}$). The presented procedure and the results can be used for a ducted fan design for an electric powered aircraft.

LIST OF SYMBOLS

a Speed of sound $[\mathrm{m\,s^{-1}}]$
A Cross-section area of a duct $[\mathrm{m^2}]$
c_p Specific heat at constant pressure $[\mathrm{J\,kg^{-1}\,K^{-1}}]$
D_1 Fan diameter $[\mathrm{m}]$
L Duct length $[\mathrm{m}]$
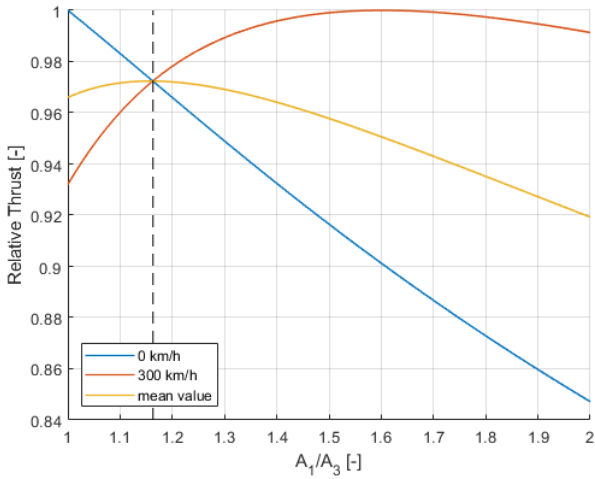
FIGURE 18. Dependence of relative thrust on nozzle contraction ratio A_1/A_3 at flight speed 0 and $300\,\mathrm{km\,h^{-1}}$. The selected nozzle contraction ratio $A_1/A_3 = 1.17$ is marked by dashed line.
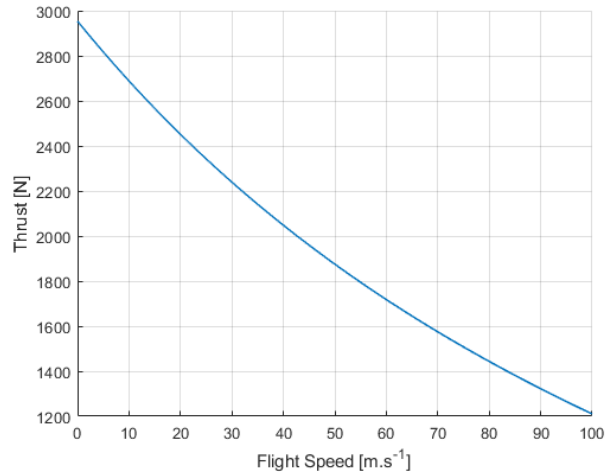
FIGURE 19. Thrust over flight speed for chosen fan parameters, i.e. $D_1 = 0.66\,\mathrm{m}$ and $A_1/A_3 = 1.17$.
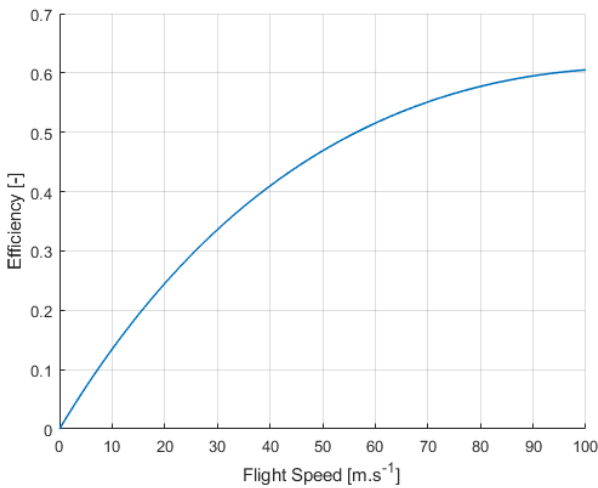
FIGURE 20. Propulsive efficiency over flight speed for chosen fan parameters, i.e. $D_1 = 0.66\,\mathrm{m}$ and $A_1/A_3 = 1.17$.
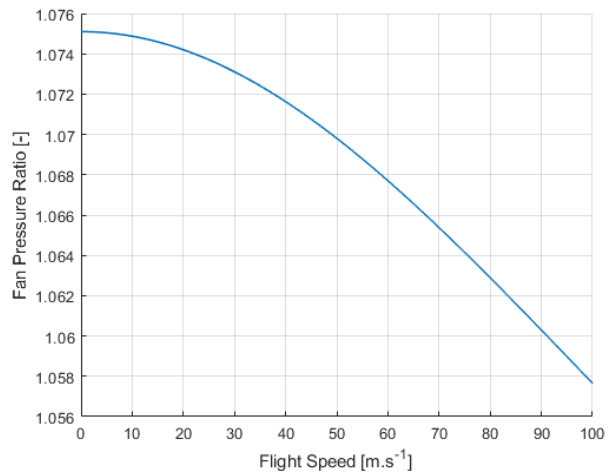
FIGURE 21. Fan pressure ratio over flight speed for chosen fan parameters, i.e. $D_1 = 0.66\,\mathrm{m}$ and $A_1/A_3 = 1.17$.
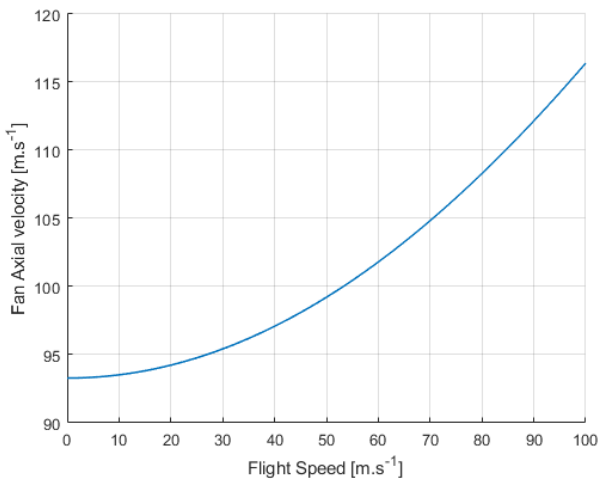
FIGURE 22. Fan axial velocity component over flight speed for chosen fan parameters, i.e. $D_1 = 0.66\,\mathrm{m}$ and $A_1/A_3 = 1.17$.
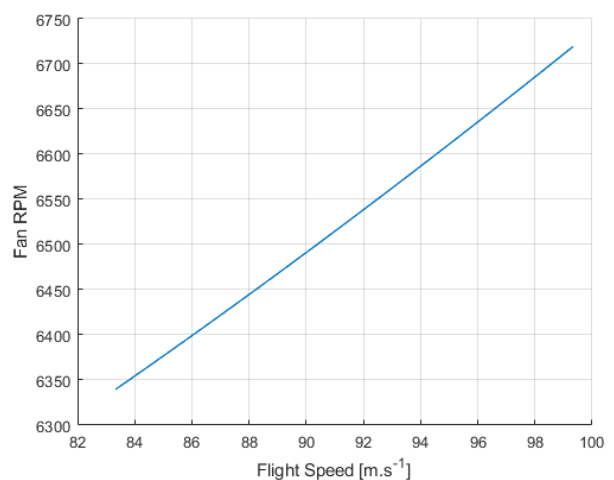
FIGURE 23. Fan RPM over flight speed for chosen fan parameters, i.e. $D_1 = 0.66\,\mathrm{m}$ and $A_1/A_3 = 1.17$.

$\dot{m}$ Air mass flow $[\mathrm{kg\,s^{-1}}]$

M Mach number

n_m Fan RPM $[\mathrm{RPM}]$

p_s Static pressure $[\mathrm{Pa}]$

p_t Total pressure $[\mathrm{Pa}]$

P Engine power $[\mathrm{W}]$

r Air specific gas constant $[\mathrm{J\,kg^{-1}\,K^{-1}}]$

T Thrust $[\mathrm{N}]$

T_t Total temperature $[\mathrm{K}]$

T_s Static temperature $[\mathrm{K}]$

v Velocity $[\mathrm{m\,s^{-1}}]$

η Efficiency

ζ Pressure loss coefficient

κ Ratio of specific heats

λ Wall friction factor

Π_{12} Fan Pressure ratio

ρ Air density $[\mathrm{kg\,m^{-3}}]$

(ρv) Flow density $[\mathrm{kg\,m^{-2}\,s^{-1}}]$

$(\rho v)_c$ Critical flow density $[\mathrm{kg\,m^{-2}\,s^{-1}}]$

ACKNOWLEDGEMENTS

REFERENCES

[1] M. Hepperle. Electric flight – Potential and limitations. *Energy Efficient Technologies and Concepts of Operation* (STO-MP-AVT-209), 2012. Accessed 2022-10-26, `https://elib.dlr.de/78726/`.

[2] Electric & hybrid-electric propulsion, 2022. Accessed 2022-10-26, `https://aerospace.honeywell.com/us/en/products-and-services/product/hardware-and-systems/electric-power/hybrid-electric-electric-propulsion`.

[3] Rolls-Royce plc. Rolls-royce advances hybrid-electric flight with new technology to lead the way in advanced air mobility, 2022. Accessed 2022-10-26, `https://www.rolls-royce.com/media/press-releases/2022/22-06-2022-rr-advances-hybrid-electric-flight-with-new-technology.aspx`.

[4] S. D. V. Weelden, D. E. Smith, B. R. Mullins. Preliminary design of a ducted fan propulsion system for general aviation aircraft. In *AIAA 34th Aerospace Sciences Meeting and Exibit*, 96-0376. `https://doi.org/10.2514/6.1996-376`.

[5] Letecká amatérská asociace ČR. UL 2 - Část I., 2019. Accessed 2022-10-26, `https://www.laacr.cz/SiteCollectionDocuments/predpisy/UL2%20%C4%8D%C3%A1st%20I_26.3.2019.pdf`.

[6] Deutscher Aero Club. Lufttüchtigkeitsforderungen für aerodynamisch gesteuerte Ultraleichtflugzeuge LTF-UL vom 15.01.2019 und Änderung vom 28.02.2019 (NfL 2-459-19), 2019. Accessed 2022-10-26, `https://www.daec.de/fileadmin/user_upload/files/2019/Luftsportgeraete_Buero/LTF/LTF-UL_2019.pdf`.

[7] N. A. Cumpsty. *Compressor Aerodynamics.* Krieger Publishing Company, 2nd edn., 2004.

[8] R. O. Bullock, I. A. Johnsen. *Aerodynamic Design of Axial Flow Compressors.* NASA-SP-36. NASA Lewis Research Center, Cleveland, OH, 1965.

[9] R. Theiner, J. Brabec. Experience with the design of ultralight airplane with unconventional powerplant. *Proceedings of the Institution of Mechanical Engineers, Part G; Journal of Aerospace Engineering* **232**(14):2721–2733, 2018. `https://doi.org/10.1177/0954410018774117`.

[10] J. Hejna. *Intake Desing for Experimental Fan.* Master's thesis, Czech Technical University in Prague, 2021. Accessed 2022-10-26, `http://hdl.handle.net/10467/96889`.

[11] S. Farokhi. *Aircraft Propulsion.* John Wiley & Sons, 2nd edn., 2014.

[12] S. Albrig. *Angewandte Strömungslehre.* Akademie-Verlag, 5th edn., 1978.